Development of A Lane Departure Monitoring and Control System

Kunsoo Huh*

School of Mechanical Engineering, Hanyang University,
17 Haengdang-Dong, Sungdong-Ku, Seoul 133-791, Korea

Daegun Hong

Department of Precision Mechanical Engineering, Hanyang University,
17 Haengdang-Dong, Sungdong-Ku, Seoul 133-791, Korea

Jeffrey L. Stein

Department of Mechanical Engineering, University of Michigan,
Ann Arbor, Michigan

The lane departure avoidance systems have been considered promising to assist human drivers in AVCS (Advanced Vehicle Control System). In this paper, a lane departure monitoring and control system is developed and evaluated in the hardware-in-the-loop simulations. This system consists of lane sensing, lane departure monitoring and active steering control subsystems. The road image is obtained based on a vision sensor and the lane parameters are estimated using image processing and Kalman Filter technique. The active steering controller for avoiding the lane departure is designed based on the lane departure metric. The proposed lane departure avoidance system is realized in a steering HILS (hardware-in-the-loop simulation) tool and its performance is evaluated with a driver in the loop.

Key Words : Lane Departure Monitoring, Lane Departure Avoidance, Lane Sensing, Active Steering Control

Nomenclature

a : Distance to the front axle from CG
b : Distance to the rear axle from CG
C_{af} and C_{ar} : Cornering stiffness of the front and rear tires
F_{yf} and F_{yr} : Lateral tire force of the front and rear tires
h_{cg} : Height of center of gravity
I_z : Moment of inertia about the z axis
K : LQR control gain
(l, w, h) : Camera origin in vehicle coordinate
m : Vehicle mass

T : Lookahead time
q_y, q_ψ, q_i, and q_p : Weighting factors
R_c : Camera rotation matrix considering the camera tile angle
R_v : Camera rotation matrix considering roll and pitch angle
r : Yaw rate
(X_c, Y_c, Z_c) : Camera coordinate
(X_g, Y_g, Z_g) : Global coordinate
(X_v, Y_v, Z_v) : Vehicle coordinate
(y, z) : Image coordinate
u : longitudinal vehicle velocity
v : Lateral vehicle speed
α_f and α_r : Tire slip angle of the front and rear tires
δ_c : Steering control input
$\delta_{c,fb}$: Feedback steering control input
$\delta_{c,ff}$: Feedforward steering control input

δ_d : Driver's steer angle
δ_{kin} : Kinematically required steer angle to follow the lane curvature
λ : Focal length of camera

1. Introduction

Lane departure warning/avoidance system is one of the key technologies for the future active-safety passenger cars. It warns the driver of drifting off the lane due to sleeping or being inattentive in a monotone environment such as straight expressways. Besides, if necessary, this system with an active steering controller can be used to control the lateral position in an unintended road departure. The lane departure warning/avoidance systems require lane sensing, lane departure monitoring and active-steering control technologies.

Lane sensing technology based on vision sensors requires little infrastructure on the highway except clear lane markers. However, they require intelligent processing algorithms in vehicles to generate reliable previewed roadway from the vision images. In order to implement the lane-sensing techniques in passenger cars, the sensing reliability and robustness should be guaranteed for the harsh environment. Various lane sensing techniques using vision sensors have been developed and reported (Takahashi and Ninomiya, 1996 ; Goldbeck and Huertgen, 1999 ; Dickmanns and Mysliwetz, 1992 ; Lin and Ulsoy, 1995 ; Huh and Park, 2002).

The lane departure monitoring of a vehicle should be judged in real-time and on-line utilizing the lane sensing results and the motion status. The typical approach for monitoring the road departure is to build rumble strips into the road edge. The rumble strips can cause the vehicle tire to vibrate as a distinctive warning, but cannot monitor in advance before the road departure actually occurs. A predictive measure of monitoring the road departure is the TLC (Time-to-Lane-Crossing) (LeBlance et al., 1996) which is defined as the time until the vehicle center crosses either edge of the roadway. The TLC is usually calculated assuming constant vehicle speed and front wheel steering angle.

Regarding the active steering control system for the lane departure avoidance, the brake-steer method with braking only had been reported (Pilutti et al., 1995), but its responses are slow and cause the unnecessary deceleration. Recently, several active steering actuators are developed such as additional electric motor and planetary gear set to the conventional steering systems (Klier and Reinelt, 2004 ; Reinelt et al., 2004 ; Asai and Kuroyanagi, 2004). These actuators allow electronically controlled superposition to the driver's steering angle and enable the advanced functions such as variable steering ratio and steering lead. In addition, they can provide interface for the vehicle dynamics and stability control systems. Moreover, the unmanned autonomous guided vehicle based on the steering controller and vision sensor is introduced (Lee et al., 2005).

In this paper, a lane departure avoidance system is developed and its performance is evaluated on a steering HILS (Hardware-in-the-loop simulations) tool. A lane sensing algorithm using vision sensors is constructed based on a lane geometry model. Its parameters such as road curvature are estimated by a Kalman filter technique and utilized to reconstruct the road geometry in the global coordinate. The FLOD (future lateral offset distance) index is proposed for the lane departure monitoring. The FLOD index is defined as the future lateral distance between the vehicle CG and the either lane of roadway after a certain look-ahead time. The well-known TLC index (LeBlance et al., 1996) and the proposed FLOD index are utilized for constructing the lane departure monitoring systems and for comparing the lane departure waring performances. The active steering control system is developed based on the LQR (Linear Quadratic Regulator) approach such that an optimal controller is designed by including lateral deviation, heading angle error, yaw rate and steering angle in the cost function. The key idea of the active-steering controller is that the driver remains in the loop and the control efforts only adjust the steering angle in addition to that given by the driver. The driver provides the primary steering commands, but only in the case of imminent lane departure, the active-steer-
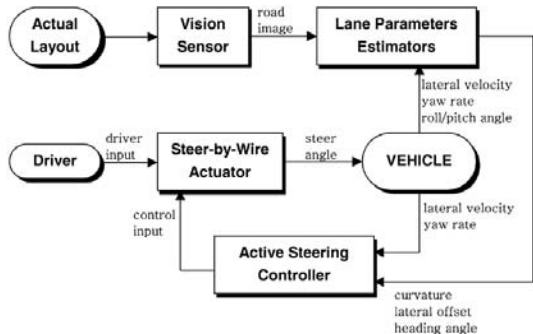
Fig. 1 Structure of lane departure avoidance system

ing controller provides additional steering angle with the steer-by-wire concept. Figure 1 shows the block diagram of the lane departure avoidance system proposed in this study. The proposed lane sensing, lane departure monitoring and active-steering control algorithms are implemented into the steering HILS (Hardware-In-the-Loop Simulation) tool.

The rest of this paper is organized as follows : Section 2 derives the lane-sensing system and Section 3 describes the active steering control system. Section 4 verifies the performance of the proposed system by HILS simulation.

2. Lane Sensing System

The structure of the proposed lane-sensing system is illustrated in Fig. 2 and consists of single camera, ROI set-up, inverse mapping and Kalman filter. A single camera acquires road scenes for the image plane. The ROI (Region Of Interest) is selected as small as possible such that the lane image processing is achieved in real-time at a low cost. The lane markers inside the selected
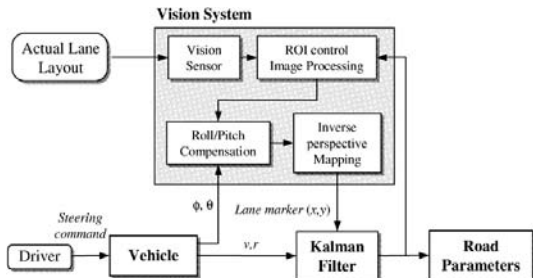
ROI are detected in the image planes. The detected lane markers in the camera coordinate are transformed into the global coordinate through the inverse perspective mapping.

Based on the transformed lane markers, the lane geometry model is constructed and its parameters are estimated utilizing the Kalman filter technique (Grewal and Andrews, 1993). In addition, the lane geometry model is used to predict the ROI locations in the incoming images.

Figure 3 shows the camera configuration and coordinate systems used in this study. Based on the assumption that road is planar, X_c in the camera coordinate can be calculated from the image coordinate and can be expressed as follows (Huh and Park, 2002) :

$$X_c = \frac{-h_{cg} - R_v(3, 1) l - R_v(3, 2) w - R_v(3, 3) h}{R(3, 1) + yR(3, 2)/\lambda + zR(3, 3)/\lambda} \quad (1)$$

where $R = R_c R_v$

● (i, j) : i-th row and j-th column element of ●

The global coordinate can be obtained from the local coordinate and the above equation using the following inverse perspective mapping relation (Huh and Park, 2002).

$$\begin{bmatrix} X_g \\ Y_g \\ Z_g \end{bmatrix} = \begin{bmatrix} 0 \\ 0 \\ h_{cg} \end{bmatrix} + R_v \left\{ \begin{bmatrix} l \\ w \\ h \end{bmatrix} + R_c \begin{bmatrix} X_c \\ y \cdot X_c/\lambda \\ z \cdot X_c/\lambda \end{bmatrix} \right\} \quad (2)$$

The horizontal lane geometry is modeled as a 2nd-order polynomial of the longitudinal distance in the global coordinate assuming that the curvature is unknown but slowly time-varying.

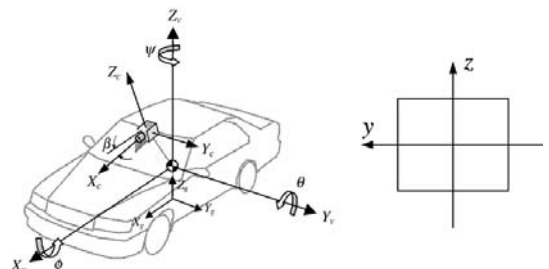$$Y_g(X_g) = c_{h0} + c_{h1}X_g + c_{h2}X_g^2/2 \quad (3)$$

Fig. 2 Structure of lane sensing system

Fig. 3 Camera Coordinates

where c_{h0} is the lateral offset, c_{h1} is the heading angle and c_{h2} is the horizontal curvature. Assuming the constant vehicle speed, the lane parameters in Eq. (3) can be described into the following dynamic equation (Lin and Ulsoy, 1995).

$$\begin{bmatrix} \dot{c}_{h0} \\ \dot{c}_{h1} \\ \dot{c}_{h2} \end{bmatrix} = \begin{bmatrix} 0 & u & 0 \\ 0 & 0 & u \\ 0 & 0 & 0 \end{bmatrix} \begin{bmatrix} c_{h0} \\ c_{h1} \\ c_{h2} \end{bmatrix} + \begin{bmatrix} -1 & 0 \\ 0 & -1 \\ 0 & 0 \end{bmatrix} \begin{bmatrix} v \\ r \end{bmatrix} \quad (4)$$

Kalman filter (Grewal and Andrews, 1993) is utilized to estimate the lane parameters in Eq. (4) based on the calculated global coordinate values.

$$Y_k = \begin{bmatrix} Y_{g1} \\ \vdots \\ Y_{gn} \end{bmatrix} = \begin{bmatrix} 1 & X_{g1} & X_{g1}^2/2 \\ \vdots & \vdots & \vdots \\ 1 & X_{gn} & X_{gn}^2/2 \end{bmatrix} \begin{bmatrix} c_{h0} \\ c_{h1} \\ c_{h2} \end{bmatrix} \quad (5)$$

where n represents the number of ROIs for the camera image. Because the proposed sensing system assumes highway lane markers, the quality of the lane marker image can be improved by predicting the possible lane marker locations. For instance, if the marker image is ambiguous or unreliable, it is unnecessary to perform the measurement update in the Kalman filter calculations. Thus, even if some lane markers are not available due to bad environmental conditions, the filter can continue to work effectively.

3. Active Steering Control System

Figure 4 shows the block diagram of the proposed active steering control system. The active steering control system is divided into two subsystems. The lane departure monitoring subsystem predicts the lane departure of a vehicle based
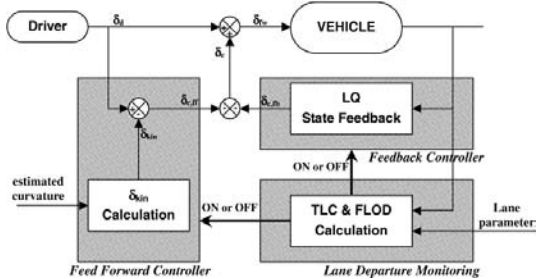

Fig. 4 Block diagram of the active steering controller

on the estimated lane parameters. The steering control subsystem calculates the additional steering angle for avoiding the lane departure. The calculated steering control angle is added to the driver's steering input using the steer-by-wire actuator or the active steering actuator.

3.1 Lane departure monitoring

The lane departure monitoring subsystem requires the information about the roadway geometry and the projected vehicle trajectory in order to judge whether the vehicle will depart the lane in a near future or not. For instance, by comparing the estimated road geometry and the predicted vehicle path, the TLC (Time-to-Lane-Crossing) index (LeBlance et al., 1996) has been introduced for the lane departure monitoring. The road geometry can be estimated from the lane sensing system as explained in the previous section. The predicted vehicle path can be obtained based on a simple vehicle model and the motion variables such as steering angle, yaw rate and longitudinal/lateral velocity. The TLC calculation results are highly dependent on the vehicle heading angel and the road curvature. If a vehicle is very close to the lane boundary and follows the lane, the TLC value is still large and the departure warning is not triggered. In this case, a lane departure may occur instantaneously by a driver's small steering input. In addition, the closer to the lane a vehicle is, the more sensitive the warning based on the TLC is to the driver's steering input.

In this paper, in order to overcome the limitation of the TLC index, the FLOD (Future Lateral Offset Distance) index is proposed utilizing the vehicle lateral offset. As illustrated in Fig. 5, the FLOD is calculated using the current vehicle lateral offset, lateral velocity and look-ahead time as follows :

$$FLOD = L_c - v_y \times T \quad (6)$$

where L_c is the current offset value in the lateral direction. The look-ahead time, T, is selected depending on the longitudinal velocity. A warning or an intervention for the lane departure avoidance is issued when the calculated FLOD falls below a threshold value.
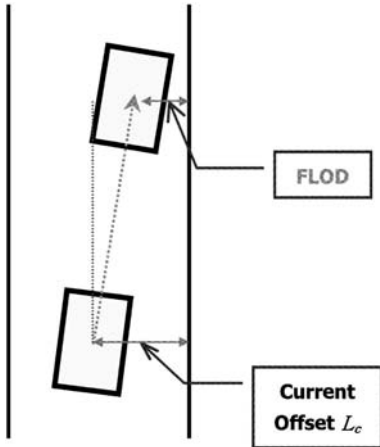
Fig. 5 Concept of the FLOD index

3.2 Steering controller design

The steering controller is activated when a vehicle is about to run off the lane. The steering controller consists of the feedforward and feedback controllers. The feedforward controller is designed to make a vehicle to follow the lane curvature and the feedback controller is designed to reduce the lateral offset error and heading angle error.

For designing the steering controller, the simplified 2 DOF vehicle model is utilized.

$$
\begin{aligned}
\dot{v} &= \left(\frac{2C_{af}+2C_{ar}}{mu}\right)v+\left(\frac{2C_{af}a-2C_{ar}b}{mu}-u\right)r \\
&\quad -\frac{2C_{af}}{m}\delta_d \\
\dot{r} &= \left(\frac{2C_{af}a-2C_{ar}b}{I_zu}\right)v+\left(\frac{2C_{af}a^2+2C_{ar}b^2}{I_zu}\right)r \\
&\quad -\frac{2C_{af}a}{I_z}\delta_d
\end{aligned} \tag{7}
$$

In designing the feed-forward controller, the required steering angle to follow the lane curvature is calculated from Eq. (7) for the steady-state cornering.

$$
\delta_{kin}=\left((a+b)+\frac{(C_{af}a-C_{ar}b)mu^2}{2(C_{af}C_{ar}(a+b))}\right)\hat{k} \tag{8}
$$

where $\hat{k}$ is the estimated lane curvature. The feed-forward steering control angle can be determined by comparing the driver's steering angle to the required steering input of Eq. (8).

$$
\delta_{c,ff}=-(\delta_d-\delta_{kin}) \tag{9}
$$

where δ_d is the driver's steering angle. The feedback controller is designed using the LQR (Linear Quadratic Regulator) approach such that the lateral offset error and heading angle error of a vehicle can be minimized in the optimal manner. The steering control input is augmented to the standard 2 DOF vehicle model as follows:

$$
\begin{aligned}
\dot{v} &= \left(\frac{2C_{af}+2C_{ar}}{mu}\right)v+\left(\frac{2C_{af}a-2C_{ar}b}{mu}-u\right)r \\
&\quad -\frac{2C_{af}}{m}\delta_d-\frac{2C_{af}}{m}\delta_c \\
\dot{r} &= \left(\frac{2C_{af}a-2C_{ar}b}{I_zu}\right)v+\left(\frac{2C_{af}a^2+2C_{ar}b^2}{I_zu}\right)r \\
&\quad -\frac{2C_{af}a}{I_z}\delta_d-\frac{2C_{af}a}{I_z}\delta_c
\end{aligned} \tag{10}
$$

A simplified roadway model is also utilized for designing the controller.

$$
\dot{y}_e=-v-u\psi_e, \quad \dot{\psi}_e=-r \tag{11}
$$

where y_e and ψ_e denote the lateral offset error and heading angle error, respectively.

By combining Eq. (10) and Eq. (11) and including the integral term of the lateral offset error, the LQR controller is constructed with five state variables.

$$
\dot{x}=A\cdot x+G\cdot\delta_d+B\cdot\delta_c \tag{12}
$$

where $x=\begin{bmatrix} v & r & y_e & \psi_e & \int y_e \end{bmatrix}^T$

$$
A=\begin{bmatrix}
\dfrac{2C_{af}+2C_{ar}}{mu} & \dfrac{2C_{af}a-2C_{ar}b}{mu} & 0 & 0 & 0 \\
\dfrac{2C_{af}a-2C_{ar}b}{I_zu} & \dfrac{2C_{af}a^2+2C_{ar}b^2}{I_zu} & 0 & 0 & 0 \\
-1 & 0 & 0 & -u & 0 \\
0 & -1 & 0 & 0 & 0 \\
0 & 0 & 1 & 0 & 0
\end{bmatrix}
$$

$$
G=\begin{bmatrix} -\dfrac{2C_{af}}{m} \\ -\dfrac{2C_{af}a}{I_z} \\ 0 \\ 0 \\ 0 \end{bmatrix}, \quad B==\begin{bmatrix} -\dfrac{2C_{af}}{m} \\ -\dfrac{2C_{af}a}{I_z} \\ 0 \\ 0 \\ 0 \end{bmatrix}
$$

Based on the above model, the optimal LQR

controller is designed by including the lateral deviation, heading angle error, integrated lateral deviation and steering control angle in the cost function.

$$J = \int_0^\infty (q_y y_e^2 + q_\psi \psi_e^2 + q_i (\int y_e)^2 + q_p \delta_c^2)\, dt \quad (13)$$

$$\delta_{c,fb} = -Kx \quad (14)$$

Finally, the active steering control input is determined by summing the feedforward control input and feedback control input.

$$\delta_c = \delta_{c,ff} + \delta_{c,fb} = -(\delta_d - \delta_{kin}) - Kx \quad (15)$$

where δ_c is the active steering control input.

   The proposed feedback controller is designed based on the 2 DOF linear vehicle model with the linear tire model in Eq. (7). However, the lateral tire force has the nonlinear characteristics such that the tire force is saturated beyond a certain tire slip angle and the tire force from the linear tire model becomes inaccurate with a large slip angle. These characteristics are very crucial because they can induce the control system unstable. In this paper, the closed-loop poles are investigated with respect to the cornering stiffness variation and uncertainty range of the cornering stiffness is determined for the stability robustness.

$$F_{yf} = (C_{af} + \Delta C_{af}) \alpha_f \\ F_{yr} = (C_{ar} + \Delta C_{ar}) \alpha_r \quad (16)$$

where ΔC_{af} and ΔC_{ar} are the cornering stiffness

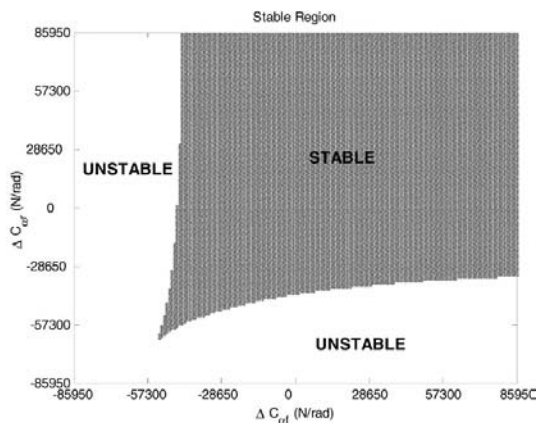changes of the front and rear tires, respectively. The stable region varies according to the vehicle speed and Fig. 6 shows the stable region in the case of 90 km/h vehicle speed. As shown in Fig. 6, the decrease in the cornering stiffness results in the saturated lateral tire force and leads to instability in the closed loop system.

4. Hils Simulation

   A steering Hardware-In-the-Loop Simulator (HILS) is built to evaluate the performance of the proposed system. As shown in Fig. 7, the HILS is composed of hardware (steering wheel, torque motor, and potentiometer) and software (vehicle simulation tool, lane sensing algorithm and active steering control system). The steering wheel is connected to the BLDC motor to generate the restoring torque and its angle is measured by the potentiometer. The real vehicle model is the modified version of the CAPC software (Ervin et al., 1995) including the 14 DOF vehicle model and nonlinear Magic Formula tire model. The proposed lane departure avoidance system is included in the software and is connected as a steer-by-wire system.
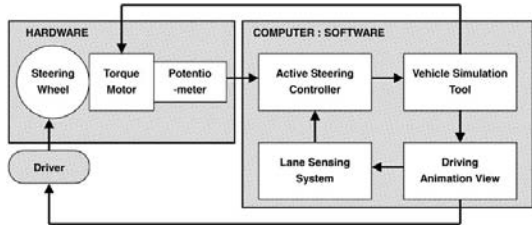
   The block diagram of the HILS simulation is illustrated in Fig. 8. The driver operates the steering wheel based on the driving animation view from the screen. The driver's steering command is measured by the potentiometer and transferred to the computer. In the computer, the lane sensing system, active steering controller and vehicle

Fig. 6 Robust stable region with respect to the cornering stiffness changes


Fig. 7 Configuration of the Steering HILS

simulation tool are worked and the driving status is viewed on the screen.

The HILS simulation with 90km/h vehicle speed is conducted in the straight road and the driver is not attentive to depart the right lane twice. Figure 9 shows the animation results from the HILS. Figure 9(a) and (b) are the animation

views for the normal driving case and lane departure warning case, respectively. Figure 9(c) and (d) illustrate the animation views where the active steering controller is activated and the vehicle is kept from the lane departure, respectively. The calculated TLC and FLOD (Future Lateral Offset Distance) values are plotted in Fig. 10 and Fig. 11, respectively. The lane departure warning results based on TLC and FLOD are compared in Fig. 12. As shown in Fig. 12, the warning trigger based on TLC is sensitive when the vehicle is close to lane. Figure 13 illustrates the trajectory of the vehicle in the HILS simulation and shows that the FLOD index is more consistent than the TLC index. It is also shown that the active controller is activated and slowly steers the vehicle back inside the lane width.

Fig. 8   Block diagram of the Steering HILS simulation
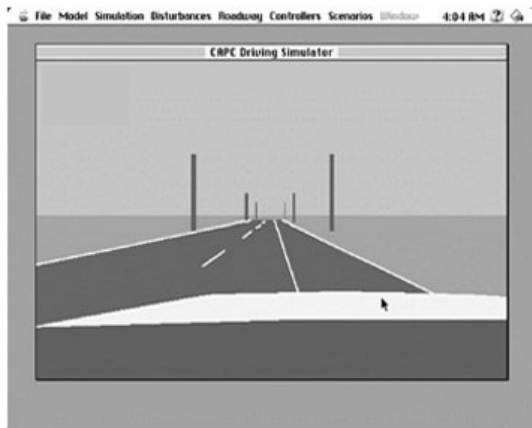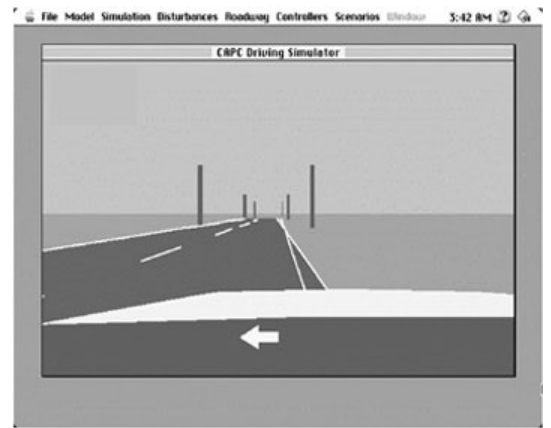
(a) Normal driving

(b) Lane departure warning
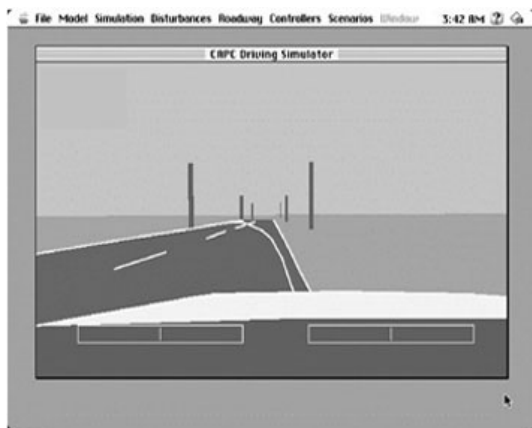
(c) Avoidance control

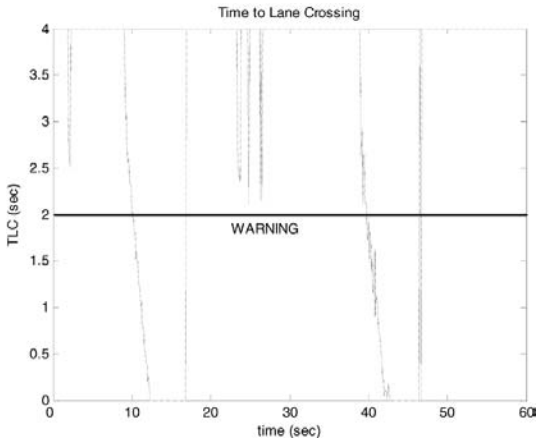(d) Normal driving after control

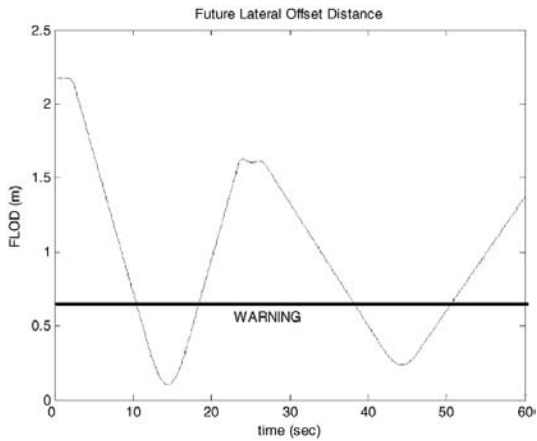**Fig. 9**   Graphical simulation display
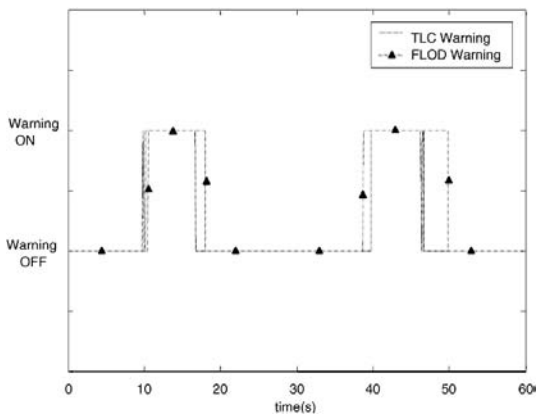
Fig. 10   TLC calculation results

Fig. 13   Vehicle trajectory

Fig. 11   FLOD calculation results

Fig. 14   Heading angle

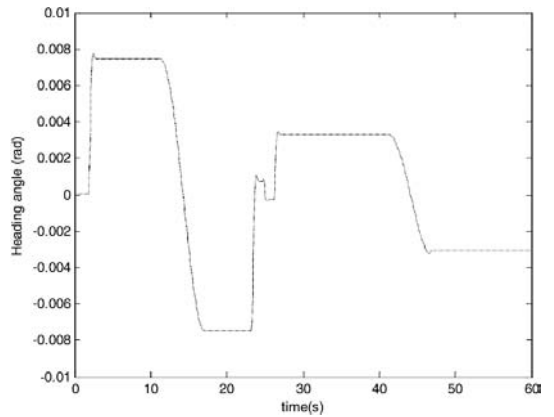**Fig. 12**   Comparison TLC with FLOD

Figure 14 shows the heading angle in the HILS simulation.

5. Conclusions

The lane departure monitoring and control system is developed based on the vision sensors and active steering controller. A lane sensing algorithm is constructed based on the model-based lane geometry recognition method. The FLOD (Future Lateral Offset Distance) index is proposed in order to represent the margin before the lane departure occurs. An active steering controller is designed using the LQR optimal control method. In the proposed system, the driver remains in the loop and the control efforts only adjust the steering angle in addition to that given by the driver. The proposed steering control system can avoid the lane departure rapidly without unnecessary deceleration using the steer-by-wire actuator or active steering actuator. The proposed the lane

departure avoidance system is implemented into the steering HILS and its performance is evaluated.

Acknowledgments

References

Asai, S. and Kuroyanagi, H., 2004, "Development of a Steer-by-Wire System with Force Feedback Using a Disturbance Observer," *SAE 2004 World Congress*, No. 2004-01-1100.

Dickmanns, E. D. and Mysliwetz, B. D., 1992, "Recursive 3-D Road and Relative Ego-state Recognition," *IEEE Transaction on PAMI*, Vol. 14, No. 2, pp. 199~213.

Ervin, R. D., Johnson, G. E., Venhovens, P. J. Th., Macdam, C. C., Ulsoy, A. G., Leblance, D. J., Lin, C. F., Peng, H., Liu, C. S., Gerber, G., DeSonia, R. and Pilutti, T. E., 1995, "The Crewmans Associate for Path Conrrol (CAPC)," Final Report for TACOM Contract DAAE07-93-C-R124, The University of Michigan Transportation Research Institute.

Goldbeck, J. and Huertgen, B., 1999, "Lane Detection and Tracking by Video Sensors," *IEEE International Conference on Intelligent Transportation Systems*, pp. 74~79.

Grewal, M. S. and Andrews, A. P. 1993, Kalman Filtering Theory and Practice, Prentice Hall, pp. 112~119.

Huh, K. and Park, Y., 2002, "Development of a Robust Lane-Sensing System Using Vision Sensors," *Proceedings of AVEC*, pp. 769~774.

Klier, W. and Reinelt, W., 2004, "Active Front Steering (Part 1): Mathematical Modeling and Parameter Estimation," *SAE 2004 World Congress*, No. 2004-01-1102.

LeBlance, D. J., Johnson, G. E., Venhovens, P. J. Th., Gerber, G., DeSonia, R., Ervin, R. D., Lin, C. F., Ulsoy, A. G. and Pilutti, T. E., 1996, "CAPC: An Implementation of a Road-departure Warning System," *Proc. of the IEEE Conf. on Control Applications*, pp. 590~595.

Lee, Y., Suh, J., Lee, J. and Lee, K., 2005, "An Adaptive Control of an Autonomous Guided Vehicle System Using Cell-Mediated Immune Algorithm Controller and Vision Sensor," *Journal of Mechanical Science and Technology*, Vol. 19, No. 1, pp. 28~39.

Lin, C. F. and Ulsoy, A. G., 1995, "Lane Geometry Reconstruction: Least Square Curve Fit Versus Kalman Filter," *ASME Advanced Automotive Technologies*, DSC-Vol. 56/DE-Vol. 86, pp. 63~70.

Pilutti, T. E., Ulsoy, A. G. and Hrovat, D., 1995, "Vehicle Steering Intervention Through Differential Braking," *Proc. of the American Control Conference*, pp. 1667~1671.

Reinelt, W., Klier, W. and Reimann, G., 2004, "Active Front Steering (Part 2): Safety and Functionality," *SAE 2004 World Congress*, No. 2004-01-1101.

Takahashi, A. and Ninomiya, Y., 1996, "Model-Based lane recognition," *Proc. IEEE Intelligent Vehicles*, pp. 162~166.